

# Imaging Vascular Thrombosis with $^{99m}\text{Tc}$ -Labeled Fibrin $\alpha$ -Chain Peptide

Mathew L. Thakur, Venkat R. Pallela, P. Macke Consigny, Ponugoti S. Rao, Donka Vessileva-Belnikovska, and Ron Shi

*Department of Radiology, Thomas Jefferson University Hospital, Philadelphia, Pennsylvania*

An agent that permits scintigraphic detection of chronic deep venous thrombosis (DVT) or pulmonary embolism (PE) would be a welcome addition to the armamentarium of nuclear medicine. Because fibrin is the integral part of each clot, old or fresh, we hypothesized that a  $^{99m}\text{Tc}$ -labeled fibrin  $\alpha$ -chain N-terminal peptide, Gly-Pro-Arg-Pro-Pro, that binds to the C-terminal portion of the  $\gamma$ -chain of fibrin can detect DVT and PE. **Methods:** The peptide was modified to Gly-Pro-Arg-Pro-Pro-Aba-Gly-Gly-(D)-Ala-Gly to permit efficient binding of  $^{99m}\text{Tc}$  ( $^{99m}\text{Tc}$ -TP 850). The stability of the peptide was examined *in vitro* as well as *in vivo*. The ability of the agent to bind to rabbit, dog, and human fibrin and to inhibit adenosine diphosphate-induced platelet aggregation was examined. Blood clearance and 3-h tissue distribution were studied. DVT was induced in 8 rabbits using a stimulating electrode and in 2 rabbits by inserting a thrombin-soaked suture. PE was induced in 6 additional rabbits by introducing tantalum-impregnated blood clots into the right atrium, and the rabbits were radiographed to locate the emboli.  $^{99m}\text{Tc}$ -TP 850 was then injected through a lateral ear vein, and each rabbit was imaged for up to 3 h. The rabbits were then killed, the heart and lungs were dissected and radiographed and the clots were harvested so that clot-to-blood radioactivity ratios could be determined. **Results:** The peptide analog permitted efficient incorporation of  $^{99m}\text{Tc}$ , which was stable *in vitro* and *in vivo*. The blood clearance was biphasic, with an  $\alpha$  phase half-life of approximately 4 min (20%) and a  $\beta$  phase half-life of approximately 13 min (88%). The mean binding of  $^{99m}\text{Tc}$ -TP 850 to human, dog, and rabbit fibrin was  $46\% \pm 2\%$ ,  $60\% \pm 3\%$ , and  $56\% \pm 2.5\%$ , respectively, and the inhibitory concentration of 50% for dog and rabbit platelet aggregation was  $236 \mu\text{m}$  and  $167 \mu\text{m}$ , respectively. All clots, including 24-h-old pulmonary emboli, were delineated. The radioactivity associated with clots varied from 0.01 to 0.09 %ID/g, with clot-to-blood radioactivity ratios ranging from 1.2 to 12.0. However, 48-h-old pulmonary emboli had lysed and were seen neither by radiography nor by scintigraphy. **Conclusion:** A fibrin  $\alpha$ -chain, N-terminal peptide that binds to the C-terminal portion of the  $\gamma$ -chain of fibrin has been modified and labeled with  $^{99m}\text{Tc}$ . The resultant peptide is stable *in vitro* and *in vivo*; binds to human, dog, and rabbit fibrin in large quantities; and inhibits platelet aggregation. The peptide clears rapidly from the blood and delineates experimental DVT and PE in rabbits. This agent is worthy of further investigation.

**Key Words:**  $^{99m}\text{Tc}$ -fibrin  $\alpha$ -chain peptide; imaging deep venous thrombosis and pulmonary embolism;  $^{99m}\text{Tc}$ -labeled peptide

J Nucl Med 2000; 41:161–168

Received Dec. 10, 1998; revision accepted May 4, 1999.  
For correspondence or reprints contact: Mathew L. Thakur, PhD, Thomas Jefferson University Hospital, 1020 Locust St., Ste. 359 JAH, Philadelphia, PA 19107.

**D**evelopment of radioactive agents for hot spot imaging of deep venous thrombosis (DVT) and pulmonary embolism (PE) has been the subject of many investigations for more than two decades (1–5). One approach to hot spot imaging has been to radiolabel platelets, which form a major biochemically active constituent of thrombi. Many agents that target platelets have been evaluated on the assumption that radiolabeled platelets will accrete on an occult thrombus and thereby facilitate its detection by external scintigraphy. Platelets have been labeled *in vitro* using such agents as  $^{111}\text{In}$ -oxine, which internalizes and binds to platelet cytoplasmic components (1). Platelets have also been labeled *in vivo* using radiolabeled proteins or peptides that are specific for the platelet surface glycoprotein IIb/IIIa complex (2–11). Despite successes with these agents in experimental animals and some human subjects, only one agent, AcuTect, the  $^{99m}\text{Tc}$ -labeled peptide P280, has recently been approved for clinical use. In an advertisement for AcuTect, the manufacturer states that the agent is expected to detect acute but not chronic venous thrombosis. The agent is also expected to detect PE, which may harbor activated platelets only sparingly.

A second approach to hot spot imaging has been to radiolabel proteins involved in clot formation. During vessel wall injury, coagulation proteins are activated sequentially and generate the enzyme thrombin. Thrombin cleaves plasma fibrinogen into fibrin monomers, which then polymerize around the platelets and hold them in place as a clot. Fibrin therefore remains an integral part of DVT, fresh or old, whether clots are embolized in the lungs or elsewhere in the body. These factors are the primary reasons for the long popularity of  $^{125}\text{I}$ -fibrinogen for external detection of DVT (2,3,5). However, the agent is no longer available commercially.  $^{123}\text{I}$ -fibrinogen and many antifibrin monoclonal antibodies labeled with various radionuclides have also been evaluated (3). However, for many reasons, such as long circulation times or poor image quality, agents other than  $^{125}\text{I}$ -fibrinogen have not entered common nuclear medicine practice.

A third approach to hot spot imaging of DVT and PE is radiolabeling of antifibrin peptides. To the best of our knowledge, the feasibility of this approach has not been

investigated. One peptide of particular interest is the N-terminal tripeptide, H-Gly-Pro-Arg-OH, of the fibrin  $\alpha$ -chain, which Laudano and Doolittle (12) reported to be an inhibitor of fibrinogen and thrombin clotting. The investigators observed that the H-Gly-Pro-Arg-Pro-OH analog of the tripeptide was an even more potent inhibitor of fibrinogen and thrombin clots by binding to the C-terminal portion of the  $\gamma$ -chain of fibrin and preventing fibrin polymerization. More recently, Kawasaki et al. (13) prepared several more analogs and found that a pentapeptide, H-Gly-Pro-Arg-Pro-Pro-OH, had the highest activity in inhibiting fibrinogen and thrombin clots. The objective of this study was to examine whether this pentapeptide, when labeled with  $^{99m}$ Tc, would facilitate imaging of DVT and PE.

## MATERIALS AND METHODS

### Preparation of Peptide

A group of four amino acids, Gly-(D)-Ala-Gly-Gly-(GAGG), was chosen as a chelating moiety. Through their NH<sub>2</sub> groups these peptides provide an N<sub>4</sub> configuration for strong chelation of  $^{99m}$ Tc. Rather than the conventional postsynthesis conjugation, the tetrapeptide chelating moiety permitted the modification of the primary peptide at the C terminus during synthesis. Furthermore, during synthesis an additional amino acid, Aba (4-aminobutyric acid), was inserted as a spacer between the chelating moiety and the primary peptide. The purpose of inserting Aba as a spacer was to minimize any possible steric hindrance resulting from the  $^{99m}$ Tc-complex. The synthesis of this modified peptide was one hybrid process that eliminated the multistep, lengthy and frequently inefficient conjugation procedure yet provided for strong chelation of  $^{99m}$ Tc. The resultant decapeptide, Gly-Pro-Arg-Pro-Pro-Aba-Gly-Gly-(D) Ala-Gly, which has an expected molecular weight of 850, is referred to as TP 850.

The peptide was custom-synthesized (PeptidoGenic Research Co., Inc., Livermore, CA) using a solid-phase synthesizer (Shimadzu, Columbia, MD) and separated using a HALSIL silica, C<sub>18</sub>, 5- $\mu$ m preparative high-performance liquid chromatography (HPLC) column (Higgins Analytical, Inc., Mountain View, CA). Ion spray mass analysis was performed using a Sciex atmosphere pressure ionization-1 mass spectrometer (Perkin Elmer, Norwalk, CT). With this chelating moiety and facility, several peptides have been prepared and labeled with  $^{99m}$ Tc in our laboratory (14-18).

### Radiolabeling and Quality Control

Fifty micrograms TP 850 were dissolved in 10  $\mu$ L 10% acetonitrile in water; then, 200  $\mu$ L 0.1-mol/L Na<sub>2</sub>PO<sub>4</sub> were added, followed by 370-1110 MBq (10-30 mCi)  $^{99m}$ Tc in 200  $\mu$ L isotonic saline previously reduced with 100  $\mu$ g SnCl<sub>2</sub> in 10  $\mu$ L 0.05-mol/L HCl. Lately, with a new batch of high-purity SnCl<sub>2</sub> (Sigma Chemicals, St. Louis, MO), we have been able to reduce the SnCl<sub>2</sub> to 10  $\mu$ g. The reaction mixture was then incubated for 30 min in a boiling water bath. The product was examined using a high-performance liquid chromatograph (Rainin, Emeryville, CA) with a reverse-phase C<sub>18</sub> column and gradient solvents of 0.1% trifluoroacetic acid in water (solvent A) and 0.1% trifluoroacetic acid in acetonitrile (solvent B). The gradient was such that solvent A was 90% at 0 min and solvent B was 100% at 30 min. The flow rate was 1 mL/min. The chromatograph was equipped with an ultraviolet detector set at 278 nm, a 5-cm (2-inch) NaI (Tl)  $\gamma$  counter and a rate meter.

### Stability of $^{99m}$ Tc-TP 850

The stability of the radiolabeled peptide at 22°C was examined by HPLC for up to 24 h as determined by the characteristic retention time (R<sub>t</sub>) of the radioactivity peak. The in vivo stability was examined by injecting rabbits with approximately 74 MBq (2 mCi)  $^{99m}$ Tc-TP 850, collecting their urine 3 h later and analyzing a 20- $\mu$ L portion of the urine by HPLC.

### Fibrin Binding

The ability of  $^{99m}$ Tc-TP 850 to bind to rabbit, dog, and human fibrin was examined in vitro. Institutional approval was obtained to draw human blood and to perform all animal experiments. Approximately 10 mL venous blood were obtained from a healthy human volunteer, a healthy young adult dog, and a rabbit. No anticoagulating agent was added to the blood. After the blood clotted, 1-mL serum samples from each blood sample were dispensed in four test tubes, approximately 925 kBq (25  $\mu$ Ci)  $^{99m}$ Tc-TP 850 (specific activity, ~12.6 GBq/ $\mu$ mol [0.34 Ci/ $\mu$ mol]) were added to each tube and the reagents were gently mixed. Thrombin (6 IU) was then added to the first two test tubes, and an equal volume of saline was added to the other two. The contents were gently mixed and allowed to incubate for 10 min at 37°C. The test tubes were then centrifuged at 2000g for 10 min, the supernatant was carefully removed and the fibrin clots in the first two test tubes were washed twice with 2 mL 0.9% NaCl. After centrifugation, the washing liquid was combined with the supernatant. Radioactivity associated with the clot and the supernatant was measured and calculated as the percentage total activity found in the compact fibrin clot.

### Inhibition of Platelet Aggregation

Seventeen milliliters of venous blood from a rabbit and a dog were collected in 3 mL acid citrate dextrose A and centrifuged at 180g for 10 min, and platelet-rich plasma was separated (1). Aggregation studies were performed using a model 430 aggregometer (Chrono-log Corp., Havertown, PA). For each study, increasing quantities of TP 850 and 4  $\mu$ mol/L adenosine diphosphate were added to 500  $\mu$ L platelet-rich plasma containing approximately 1.5  $\times$  10<sup>8</sup> platelets and stirred at 37°C. Aggregation in the absence of TP 850 was considered 100% aggregation, and the inhibitory concentration of 50% (IC<sub>50</sub>) was the quantity of TP 850 that inhibited aggregation by 50%.

### Blood Clearance

All animal protocols were approved by the institutional animal care and use committee. Blood clearance of the agent was examined in adult New Zealand white rabbits weighing between 3 and 3.5 kg. Each rabbit was anesthetized by an intramuscular injection of ketamine (30 mg/kg) and zylaxine (5 mg/kg). Then, a 23-gauge catheter was inserted in the artery of the right ear and connected to a Luer Lock (Burron Med., Inc., Bethlehem, PA). The patency of the catheter was maintained by the administration of 6 IU heparin per milliliter of sterile 0.9% NaCl administered through the Luer Lock. This catheter was used for drawing 0.5-mL blood samples in duplicate at 1, 5, 10, 15, and 30 min and 1, 2, and 3 h after radionuclide injection. Before each sample collection, enough blood was withdrawn to replace saline, which avoided dilution of the samples.

The marginal vein of the contralateral ear was used for injecting radioactive agents. The radioactivity in the syringe was measured before and after injection to determine the dose injected, and a suitable standard solution of  $^{99m}$ Tc was prepared. Blood samples were then weighed, radioactivity was counted and the results were

expressed as the percentage injected dose (%ID) per gram of blood and plotted as a function of time.

### Tissue Distribution Studies

Tissue samples were harvested from three rabbits 3 h after the administration of  $^{99m}\text{Tc}$ -TP 850. Tissues were weighed, and the radioactivity associated with each tissue and with a reference standard solution of  $^{99m}\text{Tc}$  prepared at the time of injection was determined. Radioactivity was expressed as %ID per gram of tissue. The results were averaged, and SD was determined.

### Inducing DVT

Each of eight adult male or female New Zealand white rabbits weighing between 3 and 3.5 kg was anesthetized as described, the right cubital vein or jugular vein was exposed and a stimulating electrode was inserted (19). The electrode was constructed from a 26-gauge stainless steel hypodermic needle bent at a 90° angle and attached to a 30-gauge, Teflon (DuPont, Wilmington, DE)-insulated, silver-coated copper wire. After insertion into the vessel, the needle was gently pulled so that it was in contact with the endothelial lining of the vessel and secured in place with a flared sleeve inserted over the copper wire. The second electrode was applied to the tongue of the rabbit. The stimulating electrode was attached to the anode, and the other electrode was applied to the cathode of a power supply. A 450- $\mu\text{A}$  current was then applied, and 10 min later 74 MBq (2 mCi)  $^{99m}\text{Tc}$ -TP 850 (specific activity, ~18.9 GBq/ $\mu\text{mol}$  [0.51 Ci/ $\mu\text{mol}$ ]) in 2 mL 0.9% NaCl solution were injected through a marginal ear vein. The radioactivity in each dose was measured before and after administration and recorded. A suitable reference solution with a known quantity of  $^{99m}\text{Tc}$  was also prepared. In two additional rabbits, thrombosis was induced by inserting a thrombin-soaked suture into a jugular vein 10 min before the administration of  $^{99m}\text{Tc}$ -TP 850. Serial gamma camera images of the rabbit, in the supine position, were then obtained for up to 4 h using a Starcam  $\gamma$  camera (General Electric Medical Systems, Milwaukee, WI) coupled to a low-energy, parallel-hole collimator. For each image, a total of 350,000 counts were collected.

### Inducing Pulmonary Embolism

PE was induced in 6 additional rabbits. Radio-opaque pulmonary emboli were prepared by drawing 0.5–0.75 mL blood through a 23-gauge butterfly needle inserted in the marginal ear vein and into a 1-mL syringe containing 15 mg tantalum powder and 6 IU thrombin. The contents of the syringe were then mixed gently, and a clot was allowed to form and harden for 20 min. The clot was removed from the syringe, and a 1-cm-long piece of the clot was drawn into a 6-French introducer sheath (Pinnacle; Medi-Tech, Watertown, MA), which was then inserted into a previously isolated jugular vein and advanced into the right atrium. The clot was flushed from the sheath with isotonic saline. The position of the tantalum containing clots was confirmed by obtaining a chest radiograph of the animals before the administration of  $^{99m}\text{Tc}$ -TP 850 and a radiograph of the excised lungs. After clot administration and radiographic confirmation of clot location,  $^{99m}\text{Tc}$ -TP 850 was injected and the rabbits were imaged as described. Four animals with PE were allowed to recover from the surgery. Two of these 4 were injected with  $^{99m}\text{Tc}$ -TP 850 24 h later, and the other 2 were injected with  $^{99m}\text{Tc}$ -TP 850 48 h later.

After the imaging for PE or DVT, each rabbit was given an intravenous injection of heparin (1000 IU) and was then killed with sodium pentobarbital (100 mg/kg). A blood sample was drawn, the

lungs and heart were excised and x-rayed and the clots were harvested. The clots and blood were weighed, the radioactivity associated with them was counted and clot-to-blood ratios were determined.

## RESULTS

### Peptide Radiolabeling, Quality Control, and Stability

HPLC analysis showed the peptide to be more than 90% pure. The expected molecular weight of the peptide was 850, and the molecular weight observed by mass spectroscopic analysis was 849.4. The proposed structure of  $^{99m}\text{Tc}$ -TP 850 is given in Figure 1, which shows that  $^{99m}\text{Tc}$  is bound to the chelating moiety with an N<sub>4</sub> configuration. The  $^{99m}\text{Tc}$  labeling consistently produced a better than 95% yield. HPLC analysis indicated that more than 90% of that activity was eluted in a single peak at an Rt of 7 min. A small quantity (<5%) of radioactivity was eluted at an Rt of 6.2 min, and any unbound  $^{99m}\text{Tc}$  was eluted at an Rt of 3.5 min. Figure 2 shows an elution profile.

The preparations of  $^{99m}\text{Tc}$ -TP 850 were stable at 22°C for 24 h. HPLC analysis of a urine sample (Fig. 2) collected 3 h after injection of  $^{99m}\text{Tc}$ -TP 850 showed that the radioactivity elution profile and Rt of the peak were similar to those of the preparation injected. This finding suggests that the small peptide was not susceptible to rapid in vivo proteolysis.

### Blood Clearance and Tissue Distribution

Blood clearance was biphasic, with an  $\alpha$  phase half-life of approximately 4 min (20%) and a  $\beta$  phase half-life of approximately 13 min (80%). Examination of the 3-h tissue distribution of  $^{99m}\text{Tc}$ -TP 850 indicated that the highest radioactivity was in the kidneys ( $0.108 \pm 0.086\text{ %ID/g}$ ), suggesting that the kidneys were the primary route of excretion. Hepatic uptake was  $0.016 \pm 0.014\text{ %ID/g}$ , and intestinal uptake was  $0.01 \pm 0.009\text{ %ID/g}$ . Uptake in the blood at that time was only  $0.007 \pm 0.004\text{ %ID/g}$ . This small proportion of radioactivity in circulating blood facilitated the imaging of vascular thrombi. Radioactivity in all other tissues was unremarkable.

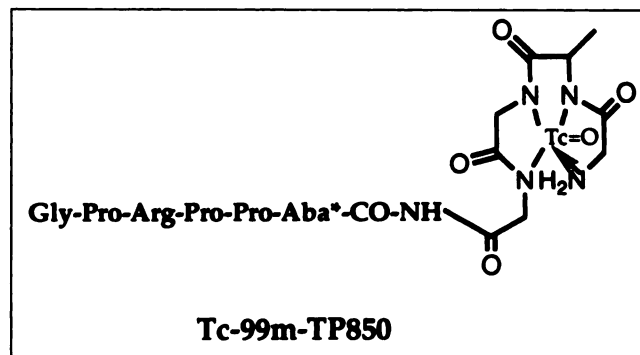
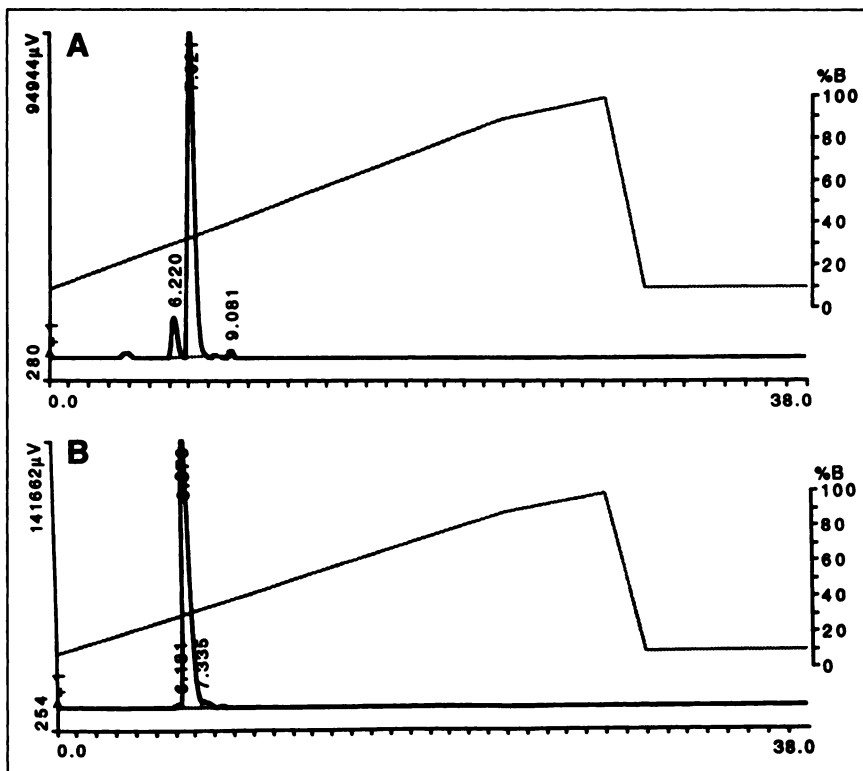


FIGURE 1. Drawing showing amino acid sequence and proposed structure of  $^{99m}\text{Tc}$ -TP 850.



**FIGURE 2.** Composite of 2 HPLC elution spectra obtained under identical solvent composition, flow rate, and column conditions. X-axis in both panels is time in minutes, and y-axis is peak radioactivity height in microvolts. Diagonal line is percentage of solvent. (A) Elution profile of  $^{99m}\text{Tc}$ -TP 850 that was injected into rabbit. (B) Elution profile of urine sample collected from rabbit 3 h later. Most radioactivity eluted in urine has Rt similar to that in sample injected. Radioactivity at Rt 4 is unbound  $^{99m}\text{Tc}$ . Small radioactivity peaks at Rt 6.2 and Rt 9.08 are considered to be caused by impurities in sample. Quantity of peptide injected was small and not detectable at 280 nm.

#### Fibrin Binding and Inhibition of Platelet Aggregation

TP 850 radioactivities associated with human, dog, and rabbit fibrin were  $42\% \pm 2\%$ ,  $60\% \pm 39\%$ , and  $56\% \pm 2.5\%$ , respectively. The  $\text{IC}_{50}$  values for dog and rabbit platelet aggregation inhibition were 236 and 167  $\mu\text{m}$ , respectively. These data justified the use of the rabbit as a model for studies with  $^{99m}\text{Tc}$ -TP 850.

#### Imaging DVT and Pulmonary Embolism

Although  $^{99m}\text{Tc}$ -TP 850 cleared rapidly from the blood, cardiac blood-pool activity was detectable in all animals at all imaging times. Radioactivity in the sinus was also detectable in all animals. This finding was consistent with the results of  $^{99m}\text{Tc}$ -TP1201 and  $^{99m}\text{Tc}$ -TP1300, two thrombospondin analogs specific for activated platelet receptors (17). Unlike these two agents, however, no  $^{99m}\text{Tc}$ -TP 850 radioactivity was seen either in the bone or in the bone cartilage. Generally, fresh thrombi and emboli could be detected by  $^{99m}\text{Tc}$ -TP 850 within 90–120 min after injection. Clots that formed spontaneously in surgical incisions or ligated vessels were also detectable. Similarly, pulmonary emboli that formed when a piece of a clot broke off or separated from a clot that was injected into the right atrium could be imaged. An example is given in Figure 3, in which an electrode-induced clot in the right foreleg, two emboli (one in each upper lobe of the lungs) and radioactivity accumulated in the incision were seen. In this animal, the foreleg clot-to-blood radioactivity ratio was 12, and the embolus-to-blood radioactivity ratios were 1.3 (left) and 2.1

(right). The radioactivities associated with the clots were 0.087, 0.006, and 0.007 %ID/g, respectively.

The clot-to-blood ratios ranged from 1.2 to 12. Many times these clots were small and could not easily be

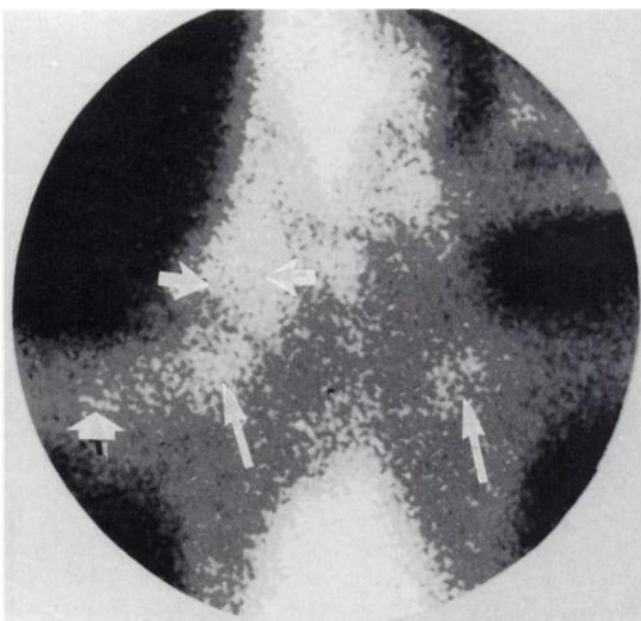


**FIGURE 3.** Anterior scintigraphic image of rabbit. Image was obtained 3 h after injection. Small thrombus induced by stimulating electrode in right foreleg (thick arrow) and PE in both upper lobes of lungs (thin long arrows) are detectable. Radioactivity accumulated in incision (thin short arrows) in right side of neck is also seen, as is radioactivity in heart and sinus.

separated from the vessel wall or adjoining fatty tissue. Similarly, tantalum was embedded in many emboli. Consequently, the weight contributed by the additional tissue or tantalum resulted in the low and variable radioactivity per unit weight of clots, emboli or thrombi.

Figure 4 shows an anterior image of a rabbit 1 h 20 min after receiving  $^{99m}\text{Tc}$ -TP 850. A clot induced in the right jugular vein by a stimulating electrode and the clot induced by the thrombin-soaked suture in the left jugular vein were detectable. The clot-to-blood ratios for these two clots were 6.5 and 3.7, and the clot radioactivity levels were 0.035 and 0.02 %ID/g. In this animal, radioactivity was also seen in the thyroid because of injection of 3.5% unbound free  $^{99m}\text{Tc}$ .

Figure 5 is an anterior  $\gamma$  camera image of a rabbit with a thrombin-soaked suture in the right jugular vein and a clot formed by stimulating electrodes in the left jugular vein. The image was obtained 150 min after injection of  $^{99m}\text{Tc}$ -TP 850. Both clots were detectable, with an electrode clot-to-blood ratio of 7.1 and a thrombin-soaked suture clot-to-blood ratio of 3.6. Inclusion of the weight of the suture in the weight of each suture clot artificially decreased the clot-to-blood radioactivity ratios. The radioactivities incorporated into the electrode and thrombin-soaked suture clots measured 0.046 and 0.024 %ID/g, respectively, of their weight.

Figure 6 shows anterior images of a rabbit with PE induced 24 h previously in both lungs. The findings were positive for clotting 1 h 15 min after injection of  $^{99m}\text{Tc}$ -TP 850. At the conclusion of *in vivo* scintigraphy, the heart and lungs were excised, spread for clarity and imaged under a

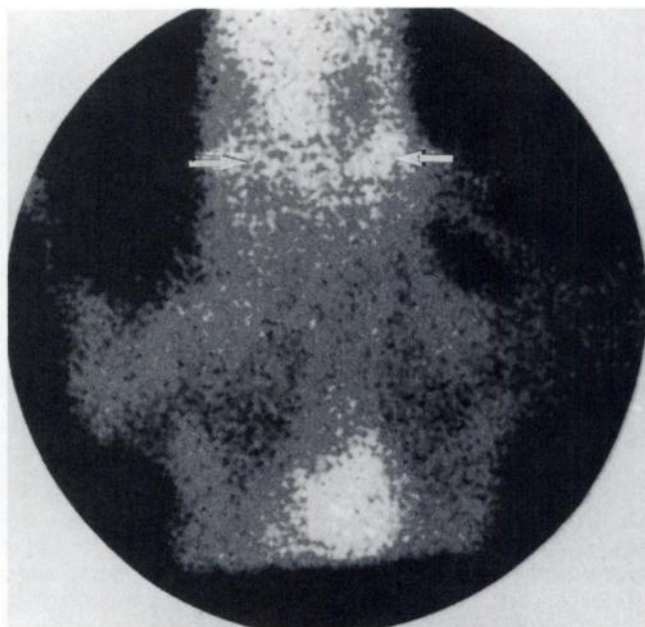


**FIGURE 5.** Anterior  $\gamma$  camera images of rabbit that was injected with 74 MBq (2 mCi)  $^{99m}\text{Tc}$ -TP 850 2 h 30 min previously. Clot caused by thrombin-soaked suture in right jugular vein and clot caused by stimulating electrode in left jugular vein are detectable (arrows). Activity caused by free  $^{99m}\text{Tc}$  in thyroid is also seen. Lower area of radioactivity is in heart.

$\gamma$  camera and with radiography. The location of the clots was corroborated. The clots were then retrieved and weighed, and the associated radioactivity was measured. The clot-to-blood ratios were 6.1 for the right clot and 3.0 for the left clot. The radioactivities in the right and left clots were 0.021 and 0.01 %ID/g, respectively.

In contrast, 48-h-old clots were detectable by neither scintigraphy nor radiography, suggesting that the clots had been lysed and had disappeared. This possibility is consistent with the high fibrinolytic activity in rabbits (20–25). The influence of anticoagulant therapy has not been studied.

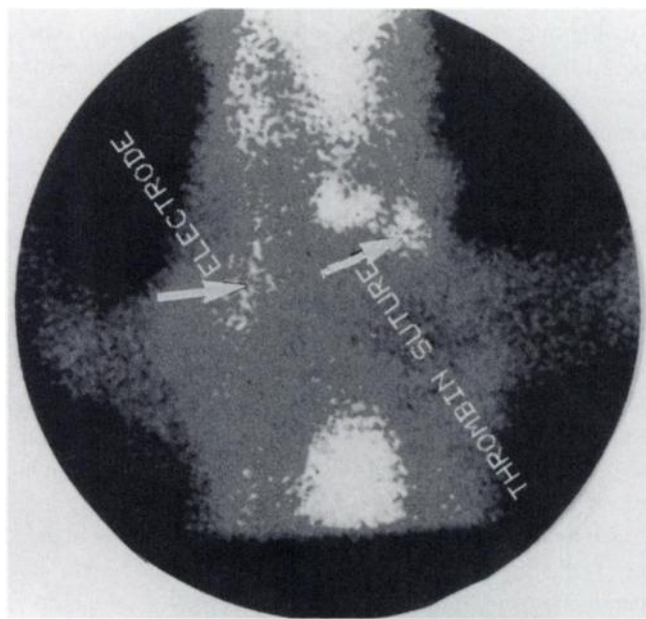


**FIGURE 4.** Anterior scintigraphic image of rabbit. Image was obtained 1 h 20 min after injection. Clot induced by stimulating electrode (clot-to-blood ratio = 6.5) and clot induced by thrombin-soaked suture (clot-to-blood ratio = 3.7) are detectable (arrows). In addition, radioactivity in heart, thyroid and paranasal sinuses can be seen. Free  $^{99m}\text{Tc}$  in preparation was approximately 3%.

## DISCUSSION

In the United States, more than 378,000 patients are hospitalized annually because of DVT, and more than 103,000, because of PE (26). These conditions contribute to more than 200,000 deaths every year. The clinical diagnosis of DVT and PE is unreliable (27,28), and PE is often underestimated, underdiagnosed, and undertreated (29). Venography is invasive, and other modalities have limitations (27,28,30). Spiral CT, MRI, and ventilation-perfusion (V/Q) scans remain the leading diagnostic tools for PE (29–36). Several interpretive pitfalls exist in assessing spiral CT images of PE (31), and MRI is not likely to replace CT (32). Although CT has better resolution and less sensitivity to moving lung artifacts, its pitfalls and the use of frequently allergenic contrast agents have led investigators to rely on V/Q scanning. However, V/Q scanning is a cold spot

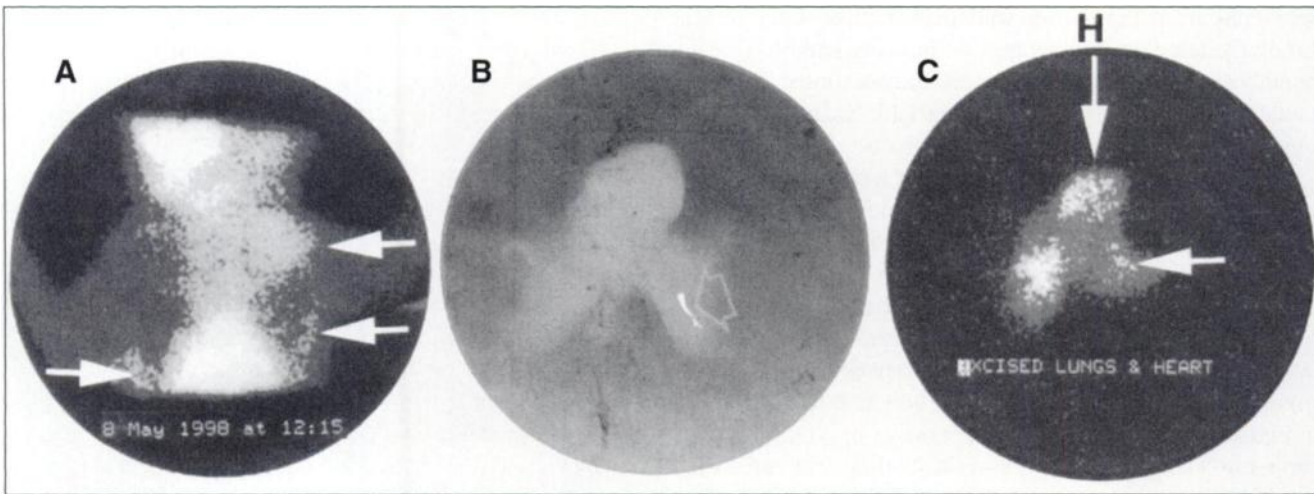


**FIGURE 6.** Composite of three images from one rabbit, in which PE was induced 24 h before intravenous administration of 88.8 MBq (2.4 mCi)  $^{99m}$ Tc-TP 850. (A) Anterior scintigraphic image obtained 1 h 15 min after injection shows abnormal accumulation of radioactivity in both lungs (arrows). Also seen is clot that formed spontaneously in left neck where incision was made for placement of PE introducer sheath. Neck clot had 3.2 times more activity than that in unit weight of blood. (B) Radiograph shows tantalum-mixed clot in left lung that corresponds to shape of clot seen scintigraphically. Clot in right lung is not seen because this clot was free of tantalum. (C) Anterior  $\gamma$  camera image of excised heart (H, arrow) and lungs shows clots in both lungs. Residual blood radioactivity is seen in heart (H).

technique and can predict only the probability of PE. Many clinicians find this type of information inadequate.

In principle, external scintigraphic techniques aided by the use of a suitable radiopharmaceutical can provide hot spot images and can fill the need for a diagnostic tool because these techniques are noninvasive and can scan the entire body without unreasonable inconvenience or added morbidity.

During the past few years, many radiopharmaceuticals have been investigated for their potential to localize DVT or PE. Because thrombi are largely composed of fibrin, platelets and other cells entrapped in the fibrin network, much attention has been drawn to the use of radioiodine-labeled fibrinogen and  $^{111}\text{In}$ -labeled platelets (37).

In many ways, radiolabeled platelets should be a simple and ideal agent, for they form a major and the most biologically active constituent of a thrombus. However, radiolabeled platelets have been less attractive, largely because their long life span (8 d) elevates background radioactivity for several days after administration. The slow clearance of radioactivity delays diagnosis because of suboptimal lesion-to-background radioactivity ratios. The platelets must also be labeled *in vitro*—a technique that requires skilled personnel (1). Furthermore, in the presence of an anticoagulant, heparin in particular, accretion of fresh platelets is impeded and  $^{111}\text{In}$ -platelet scintigraphy is less successful (37). An array of antibodies, most of them specific for the glycoprotein IIb/IIIa complex on the platelet surface, has also been investigated (29,31,32). Success with these has been limited for a variety of reasons, including lack of specificity, unfavorable pharmacokinetics and cumbersome preparation. The pros and cons of these and other agents

have been described by Knight (2), Thakur (4,5) and Koblik et al. (3).

Prompted by advancements in science and in the technology of molecular biology, recent developments in the use of radioactive agents for noninvasive diagnosis of thromboembolism are centered around  $^{99m}$ Tc-labeled peptides specific for resting or activated platelets (8–11). Peptides, which are smaller and easier to produce than monoclonal antibodies, are expected to clear more rapidly from the circulation than do radiolabeled proteins and to be less likely to induce immunologic reactions. Yet in most cases, peptides enjoy receptor specificities and binding constants as high as those of monoclonal antibodies. Because of the physical characteristic of  $^{99m}$ Tc, the  $^{99m}$ Tc-labeled peptides have become even more attractive biomolecules for diagnostic imaging than are antibodies labeled with  $^{111}\text{In}$ .  $^{99m}$ Tc is easy to obtain worldwide, is inexpensive, and decays with  $\gamma$ -ray energy (140 keV, 90%), which can be detected efficiently by planar or tomographic  $\gamma$  cameras.  $^{99m}$ Tc has a half-life (6 h) that is long enough for completion of examinations before radioactive decay becomes excessive, yet not so long that patients receive too high a dose of radiation.

All peptides evaluated thus far are specific for the platelet glycoprotein IIb/IIIa complex (8–11). Among them, one peptide,  $^{99m}$ Tc-P280, (9) was recently approved by the Food and Drug Administration under the trade name AcuTect. In an advertisement, the manufacturer describes the peptide as being expected to detect only acute thrombi, not old clots or PE. We believe a primary reason for this expectation is physiologic, in that fresh platelets, to which AcuTect may bind *in vivo*, seldom accumulate in chronic clots or PE. The

problem therefore needs a different approach—one that will permit imaging of DVT as well as PE.

The coagulation process generates fibrin monomers that form a substantial part of a clot. The actual quantity of fibrin may vary but generally is expected to be the same as the quantity of blood fibrinogen, which in most adults is as high as 5 g/100 g of plasma proteins (38). Because fibrin exists both on the surface of and within clots that are forming or dissolving, the development of a  $^{99m}$ Tc-labeled peptide specific for fibrin is appealing. Such agents, in principle, can target fibrin in a clot of any stage or state and show the clot reliably. For this purpose, one peptide of particular interest is the N-terminal fibrin  $\alpha$ -chain peptide H-Gly-Pro-Arg-OH, which was reported by Laudano and Doolittle (12) to be an inhibitor of fibrinogen and thrombin clotting. The  $\alpha$ -chain of fibrin begins with the same tripeptide sequence in many animal species and in humans. These investigators observed that the H-Gly-Pro-Arg-Pro-OH analog of the tripeptide was an even more potent inhibitor of fibrinogen and thrombin clotting than was the tripeptide itself, because the analog also bound to the C-terminal portion of the  $\gamma$ -chain of fibrin and prevented fibrin polymerization. More recently, Kawasaki et al. (13) prepared several more analogs and found that a pentapeptide, H-Gly-Pro-Arg-Pro-Pro-OH, had the highest activity in inhibiting fibrinogen and thrombin clotting.

Peptides chosen for scintigraphy are modified before they are radiolabeled so that the radiolabeling will be efficient. Most commonly, the presynthesized peptides are conjugated with a metal chelating agent. In this multistep process, peptide functional groups are blocked, chelating agents are conjugated and excess reagents are eliminated. The functional groups from the product are then deblocked, the product is separated using preparative HPLC and the required product is identified by mass spectroscopic analysis. The procedure not only is time consuming but also can frequently be inefficient.

The hybrid peptide technique that we developed to label the peptide with  $^{99m}$ Tc is simple and efficient and eliminates drawbacks. The results of these studies on inhibition of fibrin clot binding and platelet aggregation presented in this article support the notion that these modifications do not compromise the biologic activity of the peptide. These results are consistent with previous findings using biologically active peptides (17,18).

The degree of  $^{99m}$ Tc-TP 850 binding to rabbit fibrin and the  $IC_{50}$  value of  $^{99m}$ Tc-TP 850 for inhibition of rabbit platelet aggregation were high enough to justify the use of rabbits as a model for imaging experimental clots and PE. All clots, whether formed by vessel wall injury, a stimulating electrode or thrombin-soaked sutures implanted in the jugular vein, were detectable by  $\gamma$  camera scintigraphy. In general, the clots were small and their radioactivities varied from 0.01 to 0.087 %ID/g. This variability was probably caused by the presence of nonradioactive tissue or tantalum that was not separated but contributed to the weight of the

clots. However, neither the proportion of radioactivity incorporated into the clots nor the variation of this proportion is uncommon in such animal experiments (7,9,17). Despite the relatively small proportion of radioactivity, the clots were detectable at approximately 90 min after injection.

Radioactivity uptake by pulmonary emboli was considerably higher for  $^{99m}$ Tc-TP 850 than for at least two previously evaluated  $^{99m}$ Tc-labeled peptides specific for activated platelets (17). With  $^{99m}$ Tc-TP 850, all emboli were detected except those that had lysed spontaneously 48 h after placement. Because the clots that disappeared at 48 h had been impregnated with tantalum at the time of preparation, their disappearance was confirmed by loss of x-ray opacity. The choice of the rabbit as a model was based on supportive *in vitro* data described in the Results. However, the plasminogen concentration is more than twice as high in rabbits as in humans. The fibrinolytic activity in rabbits is therefore much higher and leads to rapid dissolution of these clots (20–22).

In principle, an antifibrin agent should be more successful than existing scintigraphic agents at imaging aged thrombi, with less susceptibility to interference by anticoagulants or thrombolytic agents, because during such treatments more fibrin may be exposed on the clot surface and blood flow around the clot may be greater. However, the true merit and practical usefulness of this agent can be proven only when it has been systematically shown to detect those cases of DVT and PE that existing scintigraphic agents cannot.

## CONCLUSION

A fibrin-binding pentapeptide, Gly-Pro-Arg-Pro-Pro, was modified and labeled with  $^{99m}$ Tc. Studies on inhibition of fibrin binding and platelet aggregation suggested that the biologic activity of the peptide was not compromised and that the rabbit was a suitable model for evaluation of the peptide *in vivo*. The agent cleared rapidly from the blood, and experimental deep venous thrombi and pulmonary emboli up to 24 h old were detectable by *in vivo* scintigraphy. In rabbits, clots older than 24 h lysed spontaneously. The peptide TP 850 is worthy of further study.

## ACKNOWLEDGMENTS

This work was supported by National Institutes of Health grant R41 HL 59769–01 and in part by Palatin Technologies, Inc., Princeton, NJ. These data were presented in part at the joint seventh World Federation in Nuclear Medicine and Biology and European Association of Nuclear Medicine congresses, held in Berlin, Germany, in August and September 1998. The authors thank Kate Musselman for preparing the manuscript.

## REFERENCES

- Thakur ML, Coleman RE, Hoist JH, Welch M. Indium-111 labeled platelets: studies on preparation and *in vivo* and *in vitro* functions. *Thromb Res.* 1976;9:345–354.

2. Knight LC. Radiopharmaceuticals for thrombus detection. *Semin Nucl Med*. 1990;20:52-67.
3. Koblik PD, DeNardo GL, Berger HJ. Current status of immunoscintigraphy in the detection of thrombosis and thromboembolism. *Semin Nucl Med*. 1989;19:221-231.
4. Thakur ML. Potential of radiolabeled antiplatelet antibodies in the detection of vascular thrombi. In: Srivastava SC, ed. *Radiolabeled Monoclonal Antibodies for Imaging and Therapy*. New York, NY: Plenum Publishing, North Atlantic Treaty Organization Advance Science Institutes series 152; 1988:831-845.
5. Thakur ML. Scintigraphic imaging of venous thrombosis: a state of the art. *Thromb Hematol Disord*. 1992;5:29-36.
6. Knight LC, Radcliffe R, Maurer AH, Rodwell JD, Alvarez VL. Thrombus imaging with Tc-99m synthetic peptides based upon the binding domain of a monoclonal antibody to activated platelets. *J Nucl Med*. 1994;35:282-288.
7. Knight LC, Maurer AH, Romano JE. Comparison of iodine-123-disintegrins for imaging thrombi and emboli in a canine model. *J Nucl Med*. 1996;37:476-482.
8. Pearson DA, Lister-James J, McBride WJ, et al. Thrombus imaging using Tc-99m labeled high potency GPIIb/IIIa receptor antagonist: chemistry and initial biological studies. *J Med Chem*. 1996;39:1372-1382.
9. Lister-James J, Vallabhajosula S, Moyer BR, et al. Pre-clinical evaluation of technetium-99m platelet receptor-binding platelet. *J Nucl Med*. 1997;38:105-111.
10. Line BR, Crane P, Lazewatsky J, et al. Phase I trial of DMP444, a new thrombus imaging agent [abstract]. *J Nucl Med*. 1996;37(suppl):117P.
11. Barrett JA, Crocker AC, Damphousse DJ, et al. Biological evaluation of <sup>99m</sup>Tc cyclic glycoprotein IIb/IIIa receptor antagonists in the canine arteriovenous shunt and deep vein thrombosis models: effects of chelators on biological properties of [<sup>99m</sup>Tc]chelator-peptide conjugates. *Bioconjug Chem*. 1996;7:203-208.
12. Laudano AP, Doolittle RF. Synthetic peptide derivatives that bind to fibrinogen and prevent the polymerization of fibrin monomers. *Proc Natl Acad Sci USA*. 1978;75:3085-3089.
13. Kawasaki K, Miyano M, Hirase K, Iwamoto M. Amino acids and peptides: part 18. Synthetic peptides related to N-terminus portion of fibrin  $\alpha$ -chain and their inhibitory effect on fibrinogen/thrombin clotting. *Chem Pharm Bull*. 1993;41:975-977.
14. Thakur ML, Pallela VR, Consigny PM. Tc-99m-TP 1201 for imaging thromboembolism [abstract]. *Radiology*. 1997;205(suppl):267P.
15. Pallela VR, Consigny PM, Shi R, Thakur ML. Imaging vascular thrombosis with Tc-99m-TP 1300 peptide derived from active domain of thrombospondin [abstract]. *J Nucl Med*. 1998;39(suppl):64P.
16. Pallela VR, Consigny PM, Shi R, Thakur ML. Tc-99m-labeled fibrin- $\alpha$ -chain peptide analog for imaging vascular thrombosis [abstract]. *Eur J Nucl Med*. 1998;25(suppl):87P.
17. Pallela VR, Thakur ML, Consigny PM, Rao PS, Vassileva-Belnikovska D, Shi R. Imaging thromboembolism with Tc-99m labeled thrombospondin receptor analogs TP-1201 and TP-1300. *Thromb Res*. 1999;93:191-202.
18. Pallela VR, Thakur ML, Chakder S, Rattan S. <sup>99m</sup>Tc-labeled vasoactive intestinal peptide receptor agonist: functional studies. *J Nucl Med*. 1999;40:352-360.
19. Leadley RJ, Humphrey WR, Erickson LA, Shebuski RJ. Inhibition of thrombus formation by endothelin-1 in canine models of arterial thrombosis. *Thromb Haemost*. 1995;74:1583-1590.
20. Didisheim P. Animal models useful in the study of thrombosis and antithrombotic agents. In: Spait TH, ed. *Progress in Hemostasis and Thrombosis*. New York, NY: Grune and Stratton; 1976:165-197.
21. Doolittle RF, Omecley JL, Surgeon DM. Species differences in the interaction of thrombin and fibrinogen. *J Biol Chem*. 1962;237:3123-3127.
22. Gallimore MJ, Nukar MV, Shaw JTB. A comparative study of the inhibitors of fibrinolysis in human, dog, and rabbit blood. *Thromb Diath Haemorrh*. 1965;14:145-158.
23. Hawkey CM. Fibrinolysis in animals. In: MacFarlane RG, ed. *The Haemostatic Mechanism in Man and Other Animals*. London, UK: Academic Press; 1979:143-150.
24. Mason RG, Read MS. Some species differences in fibrinolysis blood coagulation. *J Biomed Mater Res*. 1971;5:121-128.
25. Craig IH, Bell FP, Schwartz CJ. Thrombosis and atherosclerosis: the organization of pulmonary thromboemboli in the pig. *Exp Mol Pathol*. 1973;18:290-301.
26. Vital and Health Statistics Series 13: Data from National Health Care Survey. Hyattsville, MD: Department of Health and Human Services; 1993. Publication PHS 98-1797.
27. Burke B, Sostman D, Carroll B, Witty LA. The diagnostic approach to deep venous thrombosis. *Clin Chest Med*. 1995;16:253-268.
28. Worsley DF, Alavi A, Palevsky HI. Role of radionuclide imaging in patients with suspected pulmonary embolism. *Radiol Clin North Am*. 1993;31:849-859.
29. Janata-Schwatzek K, Weiss K, Riezinger I, Bankier A, Domanovits H, Seidler, D. Pulmonary embolism: diagnosis and treatment. *Semin Thromb Hemost*. 1996;22: 33-52.
30. Turkstra F, Koopman MMW, Buller HR. The treatment of deep venous thrombosis and pulmonary embolism. *Thromb Haemost*. 1997;78:489-496.
31. Remy Jardin M, Remy J, Artaud D, Deschildre F, Fribourg M, Beregi JP. Spiral CT of pulmonary embolism: technical considerations and interpretive pitfalls. *J Thorac Imaging*. 1997;12:103-117.
32. Roberts HC, Kauczor HU, Schweden F, Thelen M. Spiral CT of pulmonary hypertension and chronic thromboembolism. *J Thorac Imaging*. 1997;12:118-127.
33. Plemmons RM, Dooley DP, Longfield RN. Septic thrombophlebitis of the portal vein (pylephlebitis): diagnosis and management in the modern era. *Clin Infect Dis*. 1995;21:1114-1120.
34. Kumar R, McKinney P, Guna R. Perioperative prophylaxis of venous thromboembolism. *Am J Med Sci*. 1993;306:336-344.
35. Matsumoto A, Tegtmeier C. Contemporary diagnostic approaches to acute pulmonary emboli. *Radiol Clin North Am*. 1995;33:167-183.
36. Wakefield TW, Greenfield LJ. Diagnostic approaches and surgical treatment of deep venous thrombosis and pulmonary embolism. *Hematol Oncol Clin North Am*. 1993;7:1261-1267.
37. Sostman HD, Thakur ML, Zoghbi SS, et al. Influence of heparin on in vivo distribution of In-111 labeled platelets. *Invest Radiol*. 1985;20:198-202.
38. Diem K, Lentner C, eds. *Geigy Scientific Tables*. 7th ed. Basel, Switzerland: Geigy Pharmaceuticals; 1976:580.